Fourier filtering of linear and circular birefringence in cancer diagnosis

A.O. Karachevtsev, V.A. Ushenko, O.I. Olar, V. Marchuk,
N.V. Pashkovska, D. Andriychuk

Optics and Publishing Department,
Chernivtsi National University,
2 Kotsyubinsky Str., Chernivtsi, 58012, Ukraine
alexander.dubolazov@gmail.com

ABSTRACT

It has been proposed an optical model of linear and circular birefringence polycrystalline structure of biological crystallites. Method of polarizing optical mapping of anisotropic polycrystalline networks with spatial frequency filtering azimuth coordinate distributions of laser radiation polarization in Fourier- plane is analytically proved. Also was made an analytical study of the effectiveness of the method spatial-frequency selection in differentiation distributions azimuth field of laser radiation.

Keywords: polarimetry, birefringence, polycrystalline structure.

1. Introduction.

We propose following model representation the basis of the analysis of the transformation of laser radiation polycrystalline networks of biological layers [1-4]:

- consider the biological layer in the form of two-component isotropic-anisotropic structure;
- linear birefringence crystals form optical anisotropic multiplier of biological layer, which carry different spatial-frequency phase modulation between orthogonal components laser wave amplitude.

The main idea of filtration [5-20] is the space-frequency Fourier-images structure of laser images of polycrystalline biological component layer is different for its large-scale (fibrillar with superior linear birefringence) and small-scale (similar with predominant circular birefringence) components.

Therefore, by spatially filtering spatial-frequency can be selected low-frequency or high-frequency components, with help of Fourier- back-transformation could be transformed into various types of "filtered" image birefringence structures.

2. The structure of space-frequency filtered distributions of azimuth polarization of laser field, modified by anisotropic optical network

To determine the capabilities of the method Fourier-Stokes-polarimetry of spatial frequency filtering in optical diagnostics displays linear and circular birefringence [9-11] was performed. Computer simulations for example of network birefringence polycrystalline cylinders with ordered directions of optical axes.

We consider two types of model objects:

1. Object A - Network arranged circular cylinders with dual-frequency harmonic variables (low-frequency multiplier $\Delta n_1 = \Delta n_0 Sin\left(\frac{2\pi}{4X_0}x\right)$ and high-frequency multiplier $\Delta n_2 = \Delta n_0^* Sin\left(\frac{2\pi}{X_0}x\right)$) linear birefringence - Fig. 1;

2. Object B - similar network, the central five cylinders which are characterized by elevated (in three times) measure of the linear birefringence Δn_0^* - Fig. 2.

Eleventh International Conference on Correlation Optics, edited by Oleg V. Angelsky, Proc. of SPIE
Vol. 9066, 90661Z · © 2013 SPIE · CCC code: 0277-786X/13/$18 · doi: 10.1117/12.2053857

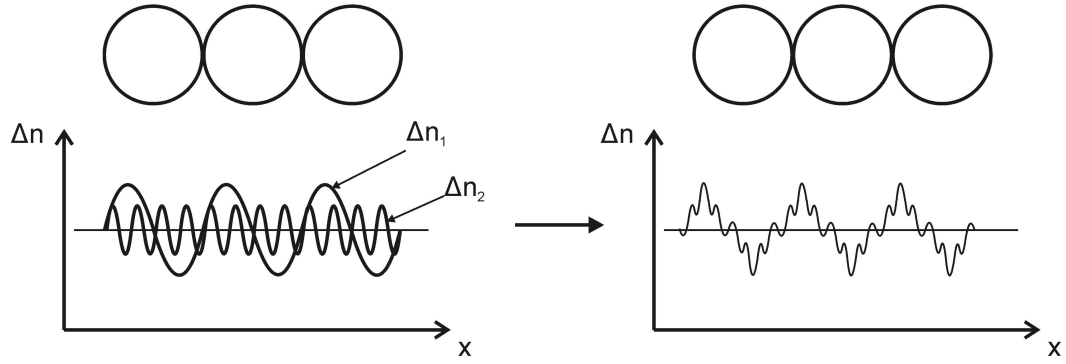

Figure. 1. Analysis of model representations (object A).

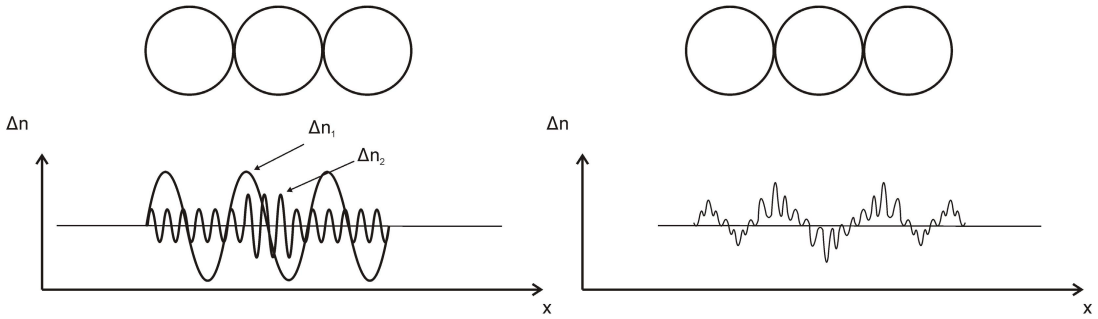

Figure. 2. Analysis of model representations (object B).

3. Spatial-frequency filtering maps azimuth of polarization images of polycrystalline networks

We used complex statistical, correlation and fractal analysis low-frequency azimuth polarization distribution both types of model network images for determination objective criterion differentiation polycrystalline structure with different level of linear birefringence [2, 5, 7].

Fig. 3; Fig. 4 illustrate spatial-frequency filtered allotment azimuth polarization large-scale component of the crystal field network with linear birefringence (a), histogram distributions of azimuth polarization values (b), autocorrelation dependence of such distributions (c), logarithmic dependences of the power spectrum ensemble of random values azimuth polarization (d).

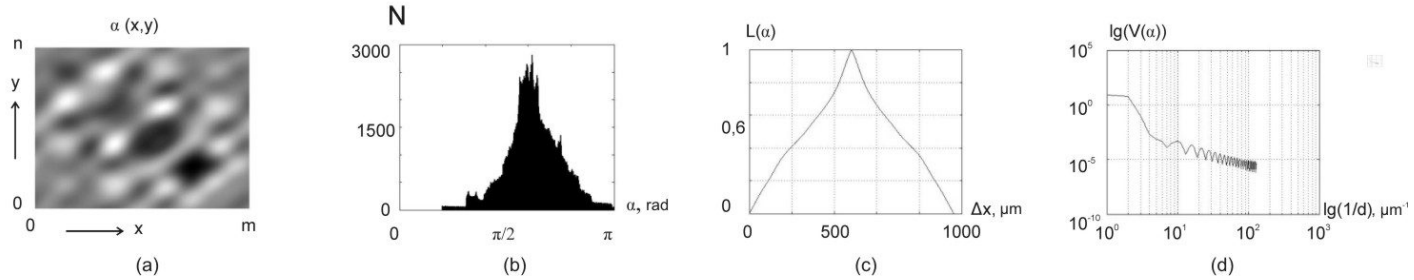

Figure. 3. Large-scale map (a), histogram (b), autocorrelation function (c), logarithmic dependence of the power spectrum (d), distribution of polarization azimuth Image polycrystalline A-type network.

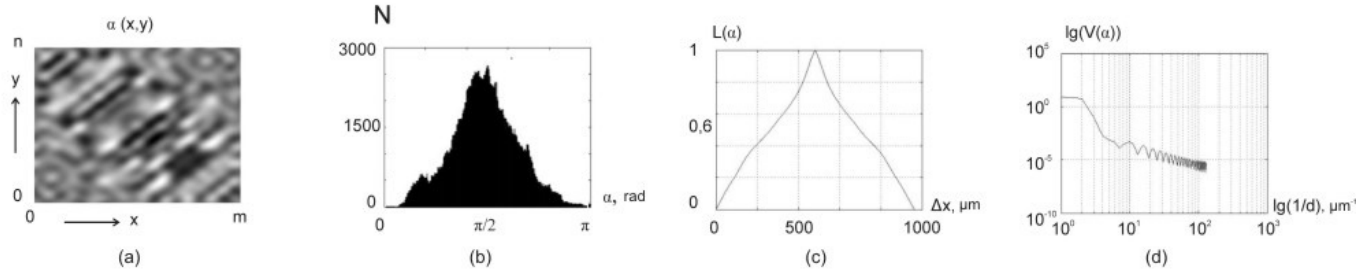

Figure. 4. Large-scale map (a), histogram (b), autocorrelation function (c), logarithmic dependence of the power spectrum (d), distribution of polarization azimuth Image polycrystalline B-type network.

As we saw, large-scale coordinate distribution maps azimuth of polarization of both types of model networks consist of a set of domains, where topographic structure which corresponding to the structure oriental directions of optical axes linear birefringence cylinders (Fig. 1; fig. 3 (a)). But, distribution random polarization azimuth values at the points of the image of polycrystalline networks are different. This fact can be related that the magnitude of linear birefringence, which forms a large scaled component polarization azimuth maps is different for different polycrystalline networks (Figure 1, Figure 2).

Quantify this difference illustrates comparative analysis of the histogram distribution of the values of the azimuth component of the large-scale polarization maps of polycrystalline azimuth model both types of networks. The histogram of distribution of the polarization parameter images polycrystalline networks with high levels of linear birefringence (type A), are characterized more asymmetrical construction (Fig. 3 (b)) in comparison with the same distribution as defined for the image of polycrystalline B-type networks (Fig. 4 (b)).

In our opinion, detected feature tied with large values of linear birefringence of the central cylinder of virtual second type network.

Optically such anisotropic building is manifested in the formation of priority among the whole set values of azimuth polarization $\alpha(x, y)$ sum of which creates a new set of extreme values corresponding histogram.

Dependence of the autocorrelation function of polarization azimuth distributions for both types of model of polycrystalline networks smoothly and monotonically decreasing (Fig. 3 (c)), Fig. 4 (c)). This indicates on a uniform structure corresponding coordinate large-scale polarization maps, generated by the mechanism of interaction of laser radiation with an ensemble of linear birefringence cylindrical crystals.

In addition, found self-similar scale construction of such maps logarithmic dependence of the power spectra of distributions characterized by polarization azimuth angle is almost the same for the whole range of variation of geometrical sizes from 2 microns to 1000 microns (Fig. 3 (d); Fig. 4 (d)).

Therefore, large-scale maps (Fig. 3 (a), Fig. 4 (a)) the value of the azimuth of polarization of polycrystalline networks arranged cylinders of both types are characterized by rather close correlation and fractal structure. The main feature of changes of linear birefringence in the range of low spatial frequencies is the transformation corresponding histogram distribution of values azimuth of polarization. Use of high-pass filter located in the center of Fourier transforms polarization azimuth maps, effectively by reverse Fourier transform to allocate small-scale component in the corresponding azimuth coordinate distributions.

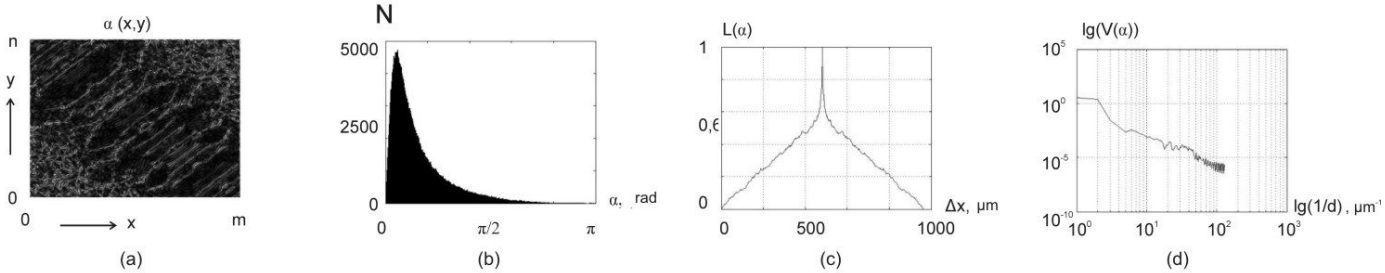

Figure. 5. Large-scale map (a), histogram (b), autocorrelation function (c), logarithmic dependence of the power spectrum (d), distribution of polarization azimuth Image polycrystalline A-type network.

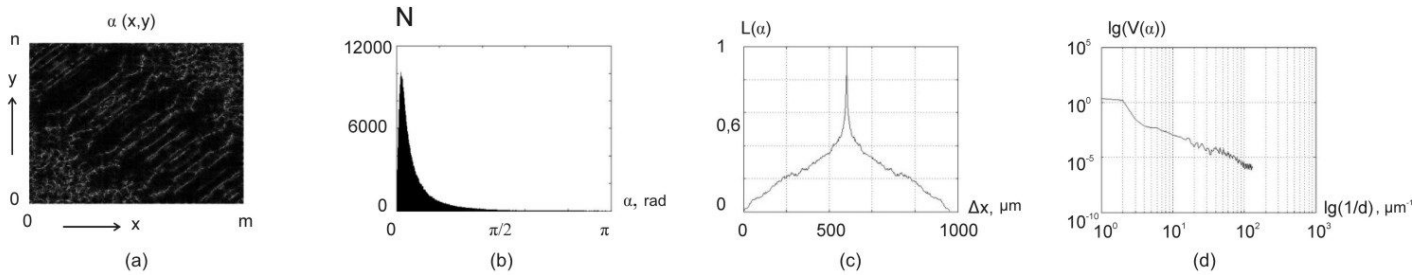

Figure. 6. Large-scale map (a), histogram (b), autocorrelation function (c), logarithmic dependence of the power spectrum (d), distribution of polarization azimuth Image polycrystalline B-type network.

Comparison of the obtained quantitative parameters that characterize the coordinate distributions of azimuth polarization (Fig. 5 (a), Fig. 6 (a)) showed the signs of change high-frequency component of the linear birefringence.

First, a significant expansion of the range of changes as well as increase the value of random values $\alpha(x, y)$ for small-scale histogram component polarization azimuth maps, generated a model network of B-type (Fig. 5 (b) Fig. 6 (b)).

Second, the increase in the depth modulation of high-frequency component of linear size birefringence leads to a more uniform distribution of random coordinate $\alpha(x, y)$ values. This trend is less rapid fall-off in half-width autocorrelation function (Fig. 5 (c), Fig. 6 (c)).

Thirdly, the growth of the value of high-frequency component in the coordinate distribution of linear birefringence cylinder network model of the second type of transformation is accompanied by large-scale self-similarity distribution $\alpha(x, y)$ (Fig. 5 (d)).

Quantitatively, this process is detectable change in approximating curves to the logarithmic dependence of the power spectra distribution of high-frequency component of polarization azimuth maps. For type A network is a single slope approximating curve $V(\rho)$ - a fractal distribution [3]. For network type B is characterized several slopes approximating curve $V(\rho)$, which indicates a multifractal distribution of building coordinate azimuth of polarization (Fig. 6 (d)).

Quantitatively, the differences between spatial frequency filtered polarization azimuth maps image modeling of polycrystalline networks of both types illustrates a set of statistical, correlation and fractal parameters listed in Tables 1 and 2.

Table 1. Statistical, correlation and self-similar structure of "large-scale" maps elasticity of polarization of polycrystalline networks birefringence cylinders both groups

Parameters	N (large-scale)	
	The type A	The type B
M_1	0,29	0,33
M_2	0,23	0,27
M_3	0,83	1,69
M_4	1,13	3,47
K_2	0,32	0,38
K_4	0,79	0,88
D	0,22	0,19

Table 2. Statistical, correlation and self-similar structure of "large-scale" maps elasticity of polarization of polycrystalline networks birefringence cylinders both groups

Parameters	N (small-scale)	
	The type A	The type B
M_1	0,074	0,087
M_2	0,12	0,14
M_3	0,56	0,81
M_4	2,06	0,58
K_2	0,12	0,28
K_4	2,68	0,71
D	0,16	0,29

Comparative analysis of spatial-frequency filtering distributions azimuth of polarization imaging model of polycrystalline networks are found diagnostically sensitive to changes in birefringence parameters:

- Statistical moments of the 3rd and 4th order orders that characterize the distribution of large-scale component of the polarization azimuth maps. The differences between the values of these parameters for both types of networks lie between 2 (M_3) to 3.5 (M_4) time;
- Statistical moments of the 2nd - 4th-order polarization azimuth distributions of small-scale component of the polarization maps image grid optically anisotropic cylinders. Distinctiveness between the values of model parameters for both types of networks lie in the range from 1.5 (M_2, M_3) to 4 (M_4) time;
- Correlation points 2nd and 4th order autocorrelation functions of coordinate distributions of small-scale component of the polarization azimuth.

Distinctiveness between the values of the parameters ranged from 2.2 (K_2) to 3.4 (K_4) time;

- Logarithmic dependence of the variance D power spectra of small-scale distributions of values azimuth component of polarization azimuth map model of polycrystalline networks of both types. Distinctiveness between the values of these parameters reach 1.7 times;
- Transformation of fractal distributions of values azimuth of polarization of small-scale component of the polarization image maps of type A network of multifractal images to network with greater depth of modulation of high-frequency component of the linear birefringence.

4. Conclusions

1. Demonstrated ability spatial- frequency filtering polarization azimuth and ellipticity maps image optically anisotropic networks with different spatial periods of the modulation of the linear birefringence.
2. Established connection between a set of statistical, correlation and spectral moments that characterize the coordinate distributions of azimuth and ellipticity of polarization of low-and high-frequency components of the image of polycrystalline networks and changes in the depth of modulation of the linear birefringence.
3. Determined diagnostically sensitive parameters to change the depth of modulation birefringence - statistical moments of the 3rd and 4th order distributions azimuth and ellipticity of large-scale component of the polarization image maps polycrystalline network.
4. Found ranges of statistical moments of the 2nd - 4th order, describing the distribution of states of polarization of the small-scale component of the image of polycrystalline networks and effective for differentiation of birefringence change layers.
5. Identified based correlation points 2nd and 4th order autocorrelation function of azimuth and ellipticity distributions of small-scale component of the polarization maps of growth modulation depth axis linear birefringence.

6. Defined large-scale self-similarity transformation scenarios distributions of states of polarization images of polycrystalline chains of type A in the multifractal distribution of polarization images optically anisotropic network type B.

REFERENCES

[1] Yasun Y. Matrix imaging of biological samples using parallel-detecting polarization-sensitive Fourier Domain Optical Cohernce tomography / Y. Yasuno, S. Makita, T. Endo, M. Itoh, T. Yatagai, M. Takahashi, C. Katada, and M. Mutoh, Shuichi Makita,Yoshiaki Yasuno, Takashi Endo, Masahide Itoh and Toyohiko Yatagai Jones // Opt. review. – 2005. – Vol. 12. – P. 146–148.

[2] Makita Shuichi. Polarization contrast imaging of biological tissues by polarization-sensitive Fourier-domain optical coherence tomography / Shuichi Makita, Yoshiaki Yasuno, Takashi Endo, Masahide Itoh, and Toyohiko Yatagai // Appl. Optics. – 2006. – Vol. 45. – P. 1142–1147.

[3] Hee M.R. Polarization-sensitive low-coherence reflectometer for birefringence characterization and ranging / M.R. Hee, D. Huang, E.A. Swanson and J.G. Fujimoto. // J. Opt. Soc. Am. B. – 1992. – V.9. – P.903-908.

[4] Yamanari Masahiro. Birefringence measurement of retinal nerve fiber layer using polarization-sensitive spectral domain optical coherence tomography with Jones matrix based analysis / Masahiro Yamanari, Masahiro Miura, Shuichi Makita, Toyohito Yatagai, Yoshiaki Yasuno // Proc. SPIE. – 2007. – Vol. 6429. – P. 496-505.

[5] Ushenko, Yu., A., Dubolazov, O., V., Karachevtsev, A., O., "Statistical structure of skin derma Mueller-matrix images in the process of cancer changes," Optical Memory and Neural Networks (Information Optics) 20(2) – P. 145-154 (2011).

[6] Ushenko, Y., O., Tomka, Y., Ya., Dubolazov, O., V., Balanetska, V., O., Karachevtsev, A., O., Angelsky,A., -P., "Wavelet-analysis for laser images of blood plasma," Advances in Electrical and Computer Engineering 11(2), P. 55-62 (2011).

[7] Balanetska, V., O., Marchuk, Yu., Karachevtsev, A., O., Ushenko, V., O., "Singular analysis of Jones-matrix images describing polycrystalline networks of biological crystals in diagnostics of cholelithiasis in its latent period," Semiconductor Physics, Quantum Electronics & Optoelectronics 14(2), P. 188-194 (2011).

[8] Dubolazov, A., V., Karachevtcev, A., O., Zabolotna, N., I., "A fractal and statistic analysis of Mueller-matrix images of phase inhomogeneous layers," Proc. SPIE 8134, P81340P4 (2011).

[9] Ushenko O., Dubolazov A., Balanets'ka V., Karachevtsev A., Sydor M., "Wavelet analysis for polarization inhomogeneous laser images of blood plasma." Proc. SPIE 8338, P. 83381H (2011).

[10] Ushenko, Y., O., Dubolazov, O., V., Karachevtsev, A., O., Gorsky, M., P., and Marchuk, Y., F., "Wavelet analysis of Fourier polarized images of the human bile," Applied Optics 51, P. 133-139 (2012).

[11] Angelsky, O., V., Hanson, S., G., Zenkova, C., Yu., Gorsky, M., P., Gorodyns'ka, N., V., "On polarization metrology (estimation) of the degree of coherence of optical waves," Optics Express 17(18), pp.15623-15634 (2009).

[12] Angel'skii, O., V., Ushenko, A., G., Arkhelyuk, A., D., Ermolenko, S., B., Burkovets, D., N.. "Scattering of laser radiation by multifractal biological structures," Optika i Spektroskopiya 88(3), 495-498 (2000).

[13] Angelsky, O., V., Ushenko, A., G., Burkovets, D., N., Ushenko, Y., A., " Polarization visualization and selection of biotissue image two-layer scattering medium," Journal of biomedical optics 10(1), P.14010 (2005).

[14] Bekshaev, A., Y., Angelsky, O., V., Hanson, S., G., and Zenkova, C., Y., "Scattering of inhomogeneous circularly polarized optical field and mechanical manifestation of the internal energy flows," Phys. Rev. A. 86, 023847 (2012).

[15] Angelsky, O., V., Polyanskii, P., V., Felde, C., V., "The emerging field of correlation optics," Optics and Photonics News 23(4), p.p.25-29 (2012).

[16] Koval, G., D., Balazyuk, V., N., Sidor, M., I., "Multiparameter correlation microscopy of blood plasma polycrystalline networks in the diagnosis of cancer tissues of female reproductive system," Proc. SPIE. 8842 (Novel Optical Systems Design and Optimization XVI), 884211 (2013).

[17] Angelsky, O.,V., Yermolenko, S.,B., Zenkova, C.,Yu., Angelskaya, A.,O., "Polarization manifestations of correlation (intrinsic coherence) of optical fields." Applied optics 47 (29), 5492-5499 (2008)

[18] Angelsky, O., Mokhun, A., Mokhun, I., Soskin, M., "The relationship between topological characteristics of component vortices and polarization singularities," Optics communications 207 (1), 57-65 (2002).

[19] Angelsky, O.,V., Burkovets, D.,N., Maksimyak, P.,P., Hanson, S.G., "Applicability of the singular-optics concept for diagnostics of random and fractal rough surfaces," Applied optics 42 (22), 4529-4540 (2003).

[20] Angel`skii, O.,V., Ushenko, O.,G., Burkovets, D.,N., Arkhelyuk, O.,D., Ushenko, Y.,A., "Polarization-correlation studies of multifractal structures in biotissues and diagnostics of their pathologic changes." LASER PHYSICS 10(5), 1136-1142 (2000).